

Low-Latency ML Inference by Grouping Correlated Data Objects and Computation

Thiago Garrett
University of Oslo
Oslo, Norway
thiagoga@ifi.uio.no

Roman Vitenberg
University of Oslo
Oslo, Norway
romanvi@ifi.uio.no

Weijia Song
Cornell University
Ithaca, USA
ws393@cornell.edu

Ken Birman
Cornell University
Ithaca, USA
ken@cs.cornell.edu

Abstract

ML inference workflows often require low latency and high throughput, yet we lack good options for addressing this need. Techniques that reduce latency in other streaming settings (such as caching and optimization-driven scheduling) are of limited value because ML data dependencies are often very large and can change dramatically depending on the triggering event. In this work, we propose a novel correlation grouping mechanism that makes it easier for developers to express application-specific data access correlations, enabling coordinated management of data objects in server clusters hosting streaming inference tasks. Experiments based on a latency-sensitive ML-based application confirm the limitations of standard techniques while showing that our solution yields dramatically better performance. The proposed mechanism is able to maintain significantly lower and more consistent latency, achieves higher node utilization as workload and scale-out increase, and yet requires only minor changes to the code implementing the application.

1 Introduction

Latency-sensitive AI-based applications are increasingly common [5]. For instance, in edge intelligence applications, devices pass captured data through Machine Learning (ML) inference pipelines [8]. Minimizing latency is the highest priority, although high throughput and efficient platform utilization remain important as secondary goals [7]. Our work starts with the observation that when these pipelines are deployed onto standard Stream Processing (SP) platforms [13], a mismatch occurs. SP systems need low latency but are typically optimized for highly parallel stateless computations and data transformations. ML inference is stateful and often context-sensitive, resulting in data dependencies that can defeat the assumptions made in SP schedulers [30].

The issue is further complicated by unpredictability. ML models depend on pretrained parameter vectors that can be large. For example, a trajectory-computing task for mobile “agents” in a traffic scene might have one set of models

trained for cars, another for bicycles, a third for pedestrians, etc. Among the vehicle models there could be one specialized for taxis, another for emergency responders, and a general-purpose model for all others. The ML logic won’t know which agents are present in the scene (and hence which objects will be needed) until runtime. Caches are too small to hold a copy of every object that might be needed, yet even a single cache miss will leave the task waiting while data is fetched. We are not aware of any SP or ML serving infrastructure with a mix of features matched to these requirements.

To assess the importance of this effect, we ran latency-sensitive ML models on both a local cluster of servers and a public cloud environment using scalable SP server-pool technologies. In all cases we observed frequent pipeline stalls stemming from data accesses that required fetching objects over the datacenter network. These stalls contribute to request backlogs that increase latency, degrade throughput and utilization, and inflate costs.

The *correlation grouping* mechanism proposed here has two main goals: (i) offer runtime mechanisms whereby developers can express application-specific knowledge about data/computation correlations in a deployment-agnostic way; and (ii) leverage this data to significantly reduce latency, particularly as workload increases and the platform scales out. The mechanism consists of three elements: developer-specified logic that will attach a string, called a *correlation key*, to each new incoming request; developer-specific code to tag stored data objects with correlation keys; and a runtime engine that makes use of correlation keys to optimize object storage and caching decisions. Leveraging correlation groups does require changes to the runtime platform, but involves minimal changes to the ML application. Benefits include enabling proactive collocation of data with computation, coordinated prefetching, and more efficient cache management.

The remainder of this work is organized as follows. Section 2 motivate our proposals by introducing a representative latency-sensitive ML-based application and identifying shortcomings of modern platforms in face of the application

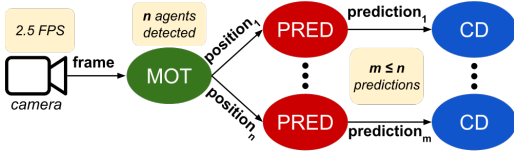


Figure 1. Computational graph of the RCP application.

data access patterns. This application is used as a running example throughout this paper. We then propose the correlation grouping mechanism in Section 3. Experimental results showing the benefits of the proposed correlation grouping mechanism are reported in Section 4. Next, we support our motivating claims regarding the shortcomings of modern platforms with experimental results reported in Section 5. Related work is presented in Section 6, and we conclude the paper in Section 7.

2 Motivation

To motivate our effort we first introduce a Real-Time Collision Prediction (RCP) application which is used as a running example in the remainder of the paper. Although we cast it in a somewhat fanciful setting, the workflow embodied in the RCP is representative of a large, important class of latency-sensitive applications [6] seen in settings such as factories, robotic warehouses and commercial retail. We then identify limitations of modern SP and ML serving platforms in face of the data access patterns showcased by the RCP application. Finally, we identify trade-offs when addressing these limitations in modern platforms.

2.1 Real-Time Collision Prediction Application

The goal of the application is to continuously predict potential imminent collisions between agents (e.g. cars, pedestrians, cyclists) in traffic intersections with a window of a few seconds. As seen in Figure 1 the RCP pipeline has three steps: multi-object tracking (MOT), trajectory prediction (PRED), and collision detection (CD). The RCP pipeline focuses on the ML, but would be deployed near cameras, signaling danger by flashing large red lights or notifying the hazard warning systems of suitably equipped vehicles. Implementation details are provided in Section 4.1.

The first step, MOT, is responsible for detecting and tracking agents in video frames received from cameras. The computation in this step consists of detecting all agents in each frame and their positions, and then matching each detected agent with its prior instance(s) if any, to determine speed and trajectory. As input, the MOT requires the current frame and the positions and features of agents found in the prior frame. Output is a set of new positions and features for all agents detected in the frame.

A separate instance of the second step, PRED, is triggered for each new position of each agent detected by the MOT step.

In this step, the next 12 positions of an agent are predicted based on the past 8 positions of that agent. Thus this step requires the current position of the agent and the previous 7 positions tracked by MOT. The output is thus a trajectory composed of 12 positions.

Each trajectory predicted by PRED triggers a separate instance of the third step, CD. This step matches the received trajectory with all other trajectories predicted so far for the same frame, in order to detect collisions. In addition to the received trajectory, this step also access all available trajectories from the same frame. For each frame, after all instances of CD have been processed, the predicted trajectories of every pair of detected agents will have been evaluated. The output of each instance of this step is a list of collisions.

2.2 Data Access Patterns and Network Overheads

Each step of the RCP application has a different data access pattern. In the MOT step, each request requires a fresh and potentially big data object – features and positions of agents in the previous frame (up to 10MB in our experiments). The nature of the input (a live stream) implies that these objects will only be used once, hence caching would be ineffective. One way to minimize overhead would be to send the object to the node where the *next* request will be processed. However, the MOT step only learns which objects it requires at runtime, after receiving the request.

PRED requires small but very fresh objects. Although agent positions can be re-used up to 7 times, there are many PRED instances for each frame, thus the overhead from cache misses can add up and become non-negligible in a time-pressured scenario. This overhead grows as more nodes are added to scale out a deployment and cache misses are more common. CD follows a similar rationale: the same trajectory is accessed many times in a short time (the same frame).

We show how significant these overheads can be in the experiments reported in Sections 4 and 5, while more details on modern platforms limitations can be found in Section 6.

2.3 Trade-offs and Limitations

It may seem that we have expressed an impossible objective, but in fact this is not the case. Developers do understand the data dependencies of their ML models, and we will show that they can express them in a simple way. Our central insight is that this is possible, and that the platform can then use the knowledge gained to improve collocation of data and computation. Existing platforms (such as standard cloud frameworks) lack the hooks required to support this capability, in part because of a presumption that such a mechanism would be in tension with other required features such as load balancing and auto-scaling. We will show that with very modest changes to the runtime infrastructure, significant latency improvements are possible even as these dynamic adaptation mechanisms do their job.

To support these claims, we deployed the RCP application twice. We first focused on a platform called Cascade, which is open source and easily extensible. Here the benefits of correlation grouping were dramatic. But then we deployed the identical RCP logic on Microsoft Azure, and ran experiments carefully following recommendations, and using Azure nodes configured for a high quality of service. Azure has fewer extension hooks than Cascade, which prevents us from implementing correlation grouping. Yet following a similar approach yields significant benefit, as shown in Section 5.

3 Correlation Grouping

We now propose the correlation grouping mechanism. As noted in the introduction, the approach has two broad objectives: (i) to offer runtime mechanisms whereby developers can express application-specific knowledge about data/computation correlations in a deployment-agnostic way; and (ii) to leverage this data to significantly reduce latency, particularly as workload increases and the platform scales out. In this section we first discuss requirements for the mechanism that arise from the limitations and trade-offs identified in Section 2. Then we introduce the mechanism per se.

3.1 Requirements

Ideally, developer-oriented mechanisms should be *deployment-agnostic*: its behavior should be predictable without deployment details. For example, although Apache Spark Resilient Distributed Datasets (RDDs) [37] offer a way to specify a list of *location preferences* when storing data, these are treated as hints. The only way to be certain that computation will be colocated with data is to hand-code a manual routing mechanism, using internal APIs to determine which servers have copies of which data items, their current load and request queue length, and resource availability.

Mechanisms such as location preferences in RDD, the *partition key* in Cosmos DB [27], and the *hash tag* in Redis [28] all facilitate collocation of correlated data. For example, data about positions of agents in the same image could be collocated in our RCP application. The cloud runtime environment then introduces further mechanisms intended to collocate stages of a pipelined computation (for example, inference MOT requests associated with the same RCP video stream) so that a single node will handle them. Other examples of collocating computation include Apache Spark Streaming *partitions* and Apache Storm *stream grouping* [33]. The problem here is that the data collocation features are decoupled from the computation collocation options, and each service uses its own way of expressing correlations. Developers need a *unified* mechanism that spans the full deployment and covers both storage placement choices and computational placement decisions.

A mechanism should also be *expressive* enough to enable the platform to track the data and computation correlations seen at runtime. For example, a single computation may require several data objects, and a single data object may be required by multiple computations. Keeping track of such correlations enables the platform to make optimized decisions regarding data and computation placement. Finally, the mechanism should be *lightweight*, i.e. the overhead introduced by the mechanism should be negligible and remain constant as the platform scales out.

3.2 Correlation Grouping Mechanism

Our goals and requirements create a complex problem, particularly in modern cloud architectures where one often finds completely independent subsystems specialized for different roles, each with its own design. In particular, storage and computation are generally treated as distinct subsystems, despite the fact that many compute nodes have substantial caches that can be viewed as a component of the storage layer. This observation became the launch point for our correlation grouping mechanism, which groups correlated objects (and hence is a storage-layer feature), yet exposes the locations of these groups so that runtime schedulers can leverage object location data in their decisions.

The next question is how correlation grouping should be expressed. A common approach that we rejected as inflexible assumes that when coding an application, developers can already anticipate the data objects required by each computational stage and declare these dependencies (e.g. using a declarative language or a SQL query) [19, 30, 40]. The platform then can parse the specification and create its own internal representation to keep track of which data objects are required by which computations. However, as seen in the RCP application, an ML model might dynamically fetch large objects based on analysis of its inputs. Such model would have an unspecifiable yet latency-critical data dependency.

The alternative approach favored here is to add a label to every request, similar in spirit to hash tags in Redis or partition keys in Azure EHs. The benefit is that labels can be computed dynamically as inputs are classified, so that (for example) an input image showing a taxi could be given a key matching various category-specific ML models and data previously saved in the platform. We call such labels *correlation keys*: each object has both a unique name (for example, a file pathname or a K/V key) and a correlation key, which would not be unique. Such an approach documents correlations between data and computation: any pair of data/computation with the same correlation key will be understood to be correlated.

The challenge to this approach is that we need to ensure that the mapping between objects and correlation keys can easily be tracked and leveraged across the whole infrastructure. This has to be done in a manner that is lightweight and that can scale to deployments with very large numbers of

applications, each with high event rate workflows, and each potentially having a unique correlation key mapping.

Although it can be implemented in different ways, the proposed correlation grouping mechanism affects two aspects of a platform: the application-level API, and the platform-level runtime engine. In the proposed mechanism, the application-level API provides developers with a way to encode application-specific knowledge, while the platform-level runtime engine makes use of the knowledge provided by developers to improve data/computation collocation, scheduling, prefetching, among other benefits discussed in Section 3.3.

The core of the correlation grouping mechanism is a function $f(r)$, which maps any request r to a set of correlation keys. We abstract different operations in a platform as requests: storing/retrieving a data object is a *data request* and requesting a computational task to be started is a *computation request*. Correlation keys are labels usually implemented as strings. The application-level API allows developers to provide the correlation grouping function f to the platform. The platform then can apply function f to any request: f extracts information from the request to generate a list of one or more keys. Application-specific knowledge is thus entirely encapsulated in f . Note that f will be available throughout the distributed service, and must return the same result for a given request no matter where it is invoked. Moreover, it is often invoked on critical paths, where blocking would be problematic. For example, in Section 4 we discuss an correlation grouping function that uses regular expressions on object keys.

In the RCP application, for example, f can map data requests of past positions of an agent a to a label “agent_a”. Computation requests that start the PRED step to predict the future trajectory of agent a can also be mapped to the same label, letting the platform know at runtime that the corresponding objects and the computation are correlated.

The platform-level runtime engine consists of a set of components distributed across the platform that makes use of the developer-provided function f . The platform must guarantee at least that: (i) the location where data objects are stored and/or cached depends on the correlation keys; and (ii) the location where computational tasks are placed depends on the correlation keys. We describe next how correlation grouping satisfies the requirements discussed in Section 3.1.

The proposed mechanism is deployment-agnostic, since function f maps requests to correlation keys according only to application-specific knowledge. The platform is then responsible to decide how to handle requests from each label according to the deployment. Since function f applies to both data and computation requests, the platform-level runtime engine is able to consider both data and computation placement in tandem. Computations and data objects are linked through labels, instead of an explicit static list of input objects or query. Developers have a great deal of flexibility when expressing data access patterns of their application.

Turning to the lightweight requirement, we argue that mechanisms such as hash tags and partition keys are potentially costly: the mapping between object keys and labels must be synchronized across the whole infrastructure, which can put a costly distributed operation such as a database update on the critical path. With correlation grouping, only function f itself must be available on all components of a platform: there is no associated replicated state.

3.3 Potential Benefits

A platform-level runtime engine can take advantage of correlation keys in many different ways.

Proactive collocation: It is possible to proactively collocate correlated data and computation by factoring correlation keys into the caching infrastructure, as well as into placement decisions of both computations on servers and objects within a scalable storage infrastructure. For example, in the RCP application, all positions from the same agent (output from the MOT step) can be stored in the same physical node where the PRED computation for that agent will take place when/if it arrives. In this example, the correlation key for all data requests and for the computation request should be the same (the identifier of the agent, for example). Collocation avoids the extra overhead of fetching input data from remote processes. Section 4 shows evidence of this benefit: as seen in Figure 5, end-to-end latency is significantly lower and more consistent when employing correlation grouping.

Prefetching: The knowledge encoded into correlation keys can also enable proactive decisions in anticipation of a future need. For example, in a multistage job a scheduler launching the first stage of a computation might also dispatch a notification that some collection of objects will be required in the second or subsequent stages. This is why our correlation key mechanism permits one object to be tagged with multiple keys: if we consider an ML computation such as RCP with a graphical structure, the output of one stage might be an input to multiple downstream stages, each with its own group of data dependencies. Using correlation keys, this would enable the platform to prefetch objects that will be needed but are not currently in cache, to transfer objects from originating node to a consuming node in anticipation of the future need, etc. Notice the similarity here to a publish-subscribe model, in which publishers might not know who the subscribers will be, and subscribers might not know their publishers. In our work, the correlation key is playing an analogous role.

Consistency: Many edge ML applications are sensitive to data sequencing. Similarly to partition keys in Azure EH, correlation keys can be used to guarantee the consistency of requests. Requests with the same correlation key may have to be handled sequentially and in order. In platforms where objects sharing the same correlation key are to be stored on the same “home nodes”, one update can be used to update the entire set as a single atomic action.

Parallelism: Requests with different correlation keys have no dependency with each other and may thus be handled in parallel. Furthermore, the correlation grouping mechanism enables a finer grain of parallelism control compared, for example, with a mechanism such as Azure EHs. In EHs, requests with different partition keys may be placed in a same partition, causing the requests to be handled sequentially, although they could be potentially have been parallelized.

4 Scaling with Correlation Grouping

In this section, we describe an implementation of the correlation grouping mechanism in Cascade [9, 31]: a state-of-the-art stream processing platform targeted at latency-sensitive ML workflows. Cascade was selected because it offered the highest baseline performance among open source platforms amenable to our methodology, enabling us to ask whether even lower latency and higher throughput might be feasible using an correlation grouping methodology.

The goal of this section is to show the benefit of correlation grouping on the end-to-end (E2E) latency of the RCP application. We evaluate the E2E latency of the application with different workloads, while also scaling out the Cascade deployment. Section 5 provides a deeper analysis on the overheads in each step of the pipeline.

4.1 RCP Application Implementation

Our experiment used the Stanford Drone Dataset (SDD) [29], which contains 60 aerial videos showing campus intersections. The videos include several types of agents (pedestrians, cars, cyclists, skateboarders, buses, and golf carts). Data source “clients” stream these videos at 2.5 FPS. All three steps are implemented in Python using the PyTorch library.

To implement the MOT step, a multi-object tracker [3] that employs YOLO5 for agent detection was used. StrongSORT [10] and OSNet [39] are used for re-identification and trajectory tracking. We selected three videos from the SDD for training (*little3*, *hyang5*, and *gates3*). Data is uncompressed, hence each frame is approximately 8MB in size. State data containing positions and features of agents detected in a frame (required to re-identify agents in the following frame) ranges from a few KBs to around 10MB depending on the number of agents in the frame. Frames from the same video must be processed sequentially, but frames from different videos can be processed in parallel by multiple instances of the MOT step. Appendix A includes plots showing the number of agents detected in each frame of each video, as well as the size of the MOT state.

The PRED step employs a trajectory prediction model, YNet [20] pretrained on the SDD data by the authors [12]. PRED requires eight consecutive positions for each agent and makes no prediction if fewer than eight are available. Position objects are small: 10s of bytes. Instances of PRED for the same agent must be processed sequentially. Instances

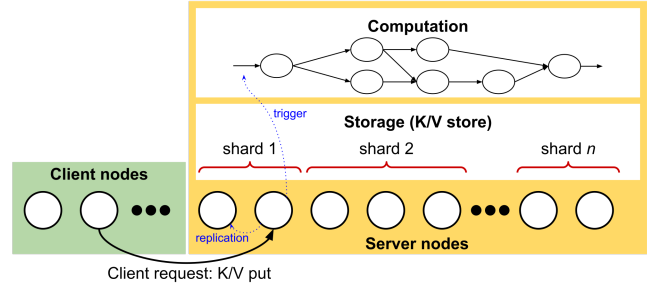


Figure 2. Cascade architecture.

triggered for different agents may be executed in parallel. Notice that the PRED workload depends not only on how many clients are streaming frames, but also on how many agents are detected in each frame.

CD consists of a simple algorithm that performs a linear interpolation on the predicted trajectories of identified agents, outputting a warning if any pair crosses. Instances of this step corresponding to the same frame and client must be processed sequentially to ensure that all pairs of trajectories will be matched with each other. Different frames (even if from the same client) may be processed in parallel.

4.2 Cascade: System Architecture

Cascade is a full-stack platform for high-speed stream processing that prioritizes low latency by hosting data and compute, avoiding copying or locking on critical data paths and leveraging acceleration technologies such as RDMA or DPDK. Backend components are implemented in C++, while client APIs are available in multiple languages (e.g. Java and Python). Cascade consists of a set of nodes interconnected in a complete network. Nodes can be clients or servers. Client nodes may issue requests to any server node. Server nodes implement two subsystems: storage and computation. Each subsystem is further described next. Figure 2 shows an overview of the system architecture.

Cascade’s storage subsystem implements a sharded Key-Value (K/V) object store. Server nodes are logically grouped into disjoint *shards* with a few nodes each. Prior to our work, each object key was hashed to determine the *home* shard for the K/V pair. Cascade supports multiples levels of persistence, but our work considered only the two in-memory mode: *trigger* requests (which cause a task to run but leave no data behind) *volatile storage* requests (which replicate an object that will then be retained in memory by all members of the home shard). Volatile storage is limited to objects that can fit within memory. In the RCP scenario, for example, object sizes ranged from a few hundred bytes to a few MBs.

Cascade’s *User-Defined Logic* (UDL) framework is responsible for executing computational tasks. The code for each task is supplied by the developer as a container or in a DLL. In either case, a self-initialization method is expected to *register*

one or more upcallable functions, each associated with a *key prefix*. On each Cascade server, an upcall will occur if that server receives a K/V pair with a matching key. For example, if a task is registered using the prefix “/RCP/taxis”, then an update to a K/V pair with key “/RCP/taxis/1234” would trigger that task. Cascade’s trigger operation will cause a single upcall to occur, on whichever node the put was sent to. Cascade’s volatile put has two possible behaviors, under developer control: it can upcall on every node in the shard that the key mapped to, or it can do the upcall on one randomly selected node within the shard.

Although a single K/V trigger or volatile put will trigger a task, once the computation is running that task can access additional objects using Cascade’s K/V *get* API. Moreover, any task can issue a trigger put or a volatile put, enabling pipelined tasks in which each stage initiates the next stage.

The potential overheads in this model are thus: (1) a P2P send operation is used to send a trigger put; (2) an atomic multicast is used to send a volatile put; (3) if a task calls get to access an object that is not homed on the node where it is executing, it must either be fetched from cache or over the network. Even with high-speed networking primitives supported by RDMA or DPDK, network transfers of large objects are costly, so Cascade must minimize the frequency of such events. Nodes have limited capacity, hence a further issue arises if the execution framework needs to enlarge the pool of compute resources. Lacking a warm-start mechanism, Cascade will incur the cost of fetching all needed objects.

Cascade supports a form of resource partitioning called an *object pool*. The basic idea is as follows: rather than treating all Cascade nodes as a single sharded service, the nodes are instead organized into groups. A single server node can belong to multiple pools. Cascade allows the developer to configure each pool with its own properties, such as the shard size to use, and the degree of data persistence the pool will offer. A persistent pool can be pinned to specific storage hardware (SSD, rotating disk, Optane, etc). A volatile pool can be pinned to host memory, GPU memory, etc. Pools are identified by pathname prefixes: if /x/y is the prefix of a volatile pool holding GPU memory objects, /x/y/z could name a tensor residing within that GPU memory.

4.3 Correlation Grouping on Cascade

Most aspects of the Cascade architecture can easily accommodate the proposed correlation grouping mechanism. As noted earlier, data and computation requests in Cascade consist of *trigger*, *put* or *get* operations. The first two are parameterized by the key and value (uninterpreted byte vector) of the object being transmitted/saved, whereas get takes a key and returns the corresponding object. We implemented function f as a regular expression, which is matched against request keys,

```

1 capi = ServiceClientAPI() # Cascade client API
2 subgroup_type = "VolatileCascadeStoreWithStringKey"
3 subgroup_index = 0
4
5 # creating object pool without correlation grouping
6 capi.create_object_pool("/no_grouping",
7                          subgroup_type, subgroup_index)
8
9 # creating object pool with correlation grouping
10 capi.create_object_pool("/grouping",
11                          subgroup_type, subgroup_index,
12                          correlation_set_regex="_[0-9]+")
13
14 # putting object in the object pool that is not grouped
15 capi.put("/no_grouping/example_1", None)
16
17 # putting object in the object pool that is grouped
18 capi.put("/grouping/example_1", None) # correlation key is '_1'

```

Figure 3. Code excerpt showing how object pools with/without grouping are created and how objects are put/get.

but with one simplification: our initial implementation limits each request to a single correlation key¹. The correlation key is a substring of the request key, composed of the characters that matched the regular expression. We employed the Hyperscan library [34] for matching regular expressions, which introduced a negligible overhead to Cascade’s critical path: according to microbenchmarks, matching the regular expressions employed in the RCP application was under 300 microseconds on average.

To implement the application-level API of the correlation grouping mechanism, we extended the Cascade client API. The extension allows developers to register regular expressions with a specified object pool. Figure 3 shows a code excerpt (in Python) with an example of how object pools are created, with and without employing correlation grouping. The only modification made to the Cascade API was the addition of the optional argument `correlation_set_regex` to the method that creates an object pool (line 12). Any put or get operation assigns an correlation key to the corresponding object by matching the object key against the regular expression registered in the corresponding object pool (line 18).

With respect to the platform-level runtime engine, we made two modifications to Cascade: (i) the mapping from key to shard within an object pool is based on the correlation key instead of the request key; and (ii) the correlation key functions and their matching expressions are registered in all nodes. As described above, Cascade previously selected the shard that will handle a request by hashing the object key supplied with the object describing the request. Our modified policy selects the shard by hashing the correlation key. Jointly, these changes ensure that all objects with the same correlation key will be stored (and replicated) in the

¹In future work we will support mappings to multiple correlation keys. A single key suffices for the RCP application, but multiple keys are likely to be important in more complex applications where the output of one compute stage is consumed by multiple follow-on stages, each with its own dependency set.

same shard, and route requests using that same correlation key to this shard.

An open question concerns whether (and how) schedulers should be extended to factor in correlation grouping considerations. Cascade is already designed to send computations to the home nodes of needed objects, or to nodes where those objects are cached: an ideal policy from our perspective.

4.4 Computing Environment

We now describe a series of experiments conducted on our local cluster. Servers in the cluster are equipped with Mellanox ConnectX-4 VPI NIC cards connected to a Mellanox SB7700 InfiniBand switch. This configuration results in a RDMA-capable 100Gbps network backbone. All servers have their clocks synchronized using PTP [11], making timestamps from different servers comparable with sub-millisecond precision. Servers have two configurations, denoted **A** and **B** in this work. Configuration **A** consists of two Intel Xeon Gold 6242 CPUs, 192 GB of memory, and an NVIDIA Tesla T4 GPU. This configuration is commonplace in Edge Cloud environments, where applications such as RCP are often deployed. Configuration **B** consists of two Intel Xeon E2690 v0 CPUs and 96 GB of memory, but no GPU. All servers run Linux kernel 5.15.0. Cascade nodes were deployed on Docker (version 24.0.6) containers hosted on the cluster servers. Containers were based on Ubuntu 22.04, with CUDA version 11.7.

Cascade was deployed with three object pools, one per step. Cascade nodes in pools responsible for MOT and PRED were deployed on containers hosted on servers with configuration **A**, since these steps require GPUs for ML inference. Clients and other Cascade nodes were deployed on containers hosted on servers with configuration **B**. In this section, we report results with a varying number of shards in each pool, as well as a varying number of nodes in each shard. Each configuration of shards/nodes is called a *layout*.

Although Cascade includes a scheduler, we configured the system to place objects and trigger computations purely by correlation key hashing. This enables us to focus on the degree to which a purely correlation grouping placement of data and computation can improve latency.

4.5 RCP Application Deployment on Cascade

Each step of the RCP application was deployed as a DLL on Cascade’s UDL framework. UDLs are loaded by each Cascade node on startup. ML models are also loaded on startup by the UDLs – all nodes have local access to models and hyperparameters. All required objects (MOT state data, agent positions and trajectory predictions) are stored/retrieved using Cascade K/V store.

Each client is responsible for a different video, and sends complete video frames at a rate of 2.5 FPS. To send a frame, a client puts an object in the K/V store with a key that will trigger a MOT task. The MOT task retrieves the state data from the previous frame, and puts a separate object for each

agent position found in the frame. Each agent position put by the MOT task triggers a PRED computation. Each PRED task first retrieves the past positions of the corresponding agent from the K/V store, and puts an object with the trajectory prediction. Each trajectory prediction triggers a CD computation, which first retrieves all trajectory predictions for the same frame available in the K/V store, and then performs the computation. The result of the collision detection is put in the K/V store. The E2E latency is the time elapsed between the client sending the frame, until the result of the last collision detection for that frame is put in the K/V store. All tasks cache in memory all objects they retrieve or create.

We employed two different workloads: single clients (*little3*, *hyang5*, and *gates3*), and three simultaneous clients (*little3 + hyang5 + gates3*). Each client send 700 frames, and we discard measurements from the first 100 frames. Each experiment is repeated three times. Cascade was completely cleared of objects and object pools before each run of each experiment, and a setup script was executed to create the necessary object pools.

We grouped requests from each step using the correlation grouping mechanism in a different way. For MOT, grouping was based on the identifier of the client, so that all frames from a same client always went to the same shard. For PRED, grouping was based on agent identifiers, and for CD it was based on both the client identifier and the frame number. Table 1 shows all the employed object pools, examples of object keys, which computations are triggered when objects are put in the corresponding object pool (if any), the regular expressions used to group requests (if any), and the resulting correlation keys from matching the regular expressions against the example keys.

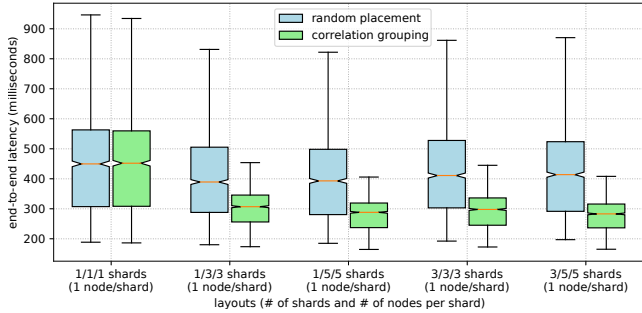
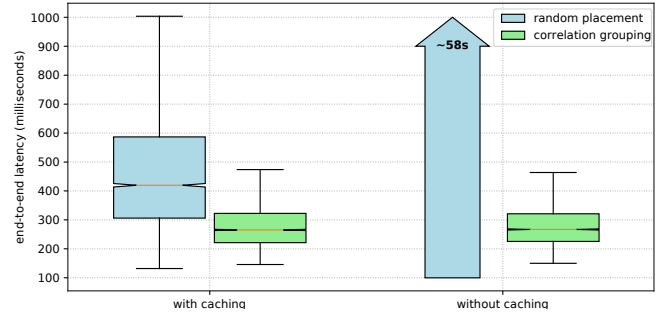
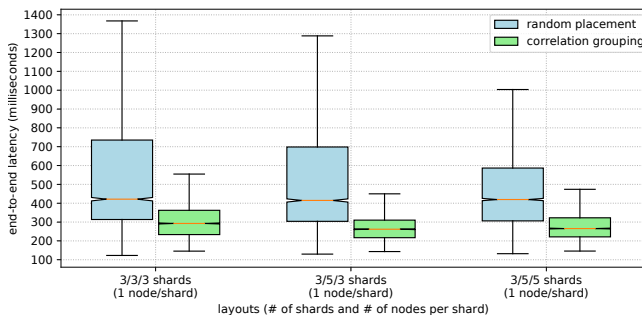
Results reported in this section compare two different placement strategies, random placement and correlation grouping. In the random placement strategy, the RCP application is executed without using correlation grouping, i.e. objects and computations are placed randomly by hashing requests keys – the standard Cascade behavior. In the correlation grouping strategy, we group requests as described above.

4.6 Results

We now report results for experiments with just one client. We varied the number of shards for MOT (1, 3), PRED (1, 3, 5) and CD (1, 3, 5). The number of nodes in each shard was 1. Figure 4 shows a box plot of the E2E latency (in milliseconds) for different layouts and placement strategies. We show only results for client *gates3* for the sake of saving space. Results for other clients followed the same pattern. It is possible to see that correlation grouping significantly decreased both median and 75th percentile latencies, except for layout 1/1/1, in which the grouping mechanism had no effect since there was only 1 shard per step. Furthermore, increasing the number of shards did not improve latency with

Table 1. Object pools, example keys, triggered steps, regular expressions, and correlation keys.

Object Pool	Example Key	Step	Regex	Correlation Key
/collision/tracking/cameras	/collision/tracking/cameras/little3_42	MOT	/[a-zA-Z0-9]+_	/little3_
/collision/tracking/states	/collision/tracking/states/little3_42	-	/[a-zA-Z0-9]+_	/little3_
/collision/tracking/agent_position	/collision/tracking/agent_position/little3_7_42	PRED	/[a-zA-Z0-9]+_[0-9]+_	/little3_7_
/collision/prediction/agent_prediction	/collision/prediction/agent_prediction/little3_42_7	CD	/[a-zA-Z0-9]+_[0-9]+_	/little3_42_
/collision/detection	/collision/detection/little3_42_7_5	-	-	-

**Figure 4.** E2E latency for *gates3* on Cascade.**Figure 6.** E2E latency with/without caching on Cascade.**Figure 5.** E2E latency for three clients on Cascade.

the random placement strategy. In fact, both the median and percentile latencies slightly increased as more shards were added: fetching overhead increased, due to more cache misses.

We now increase the workload to three simultaneous clients. Figure 5 shows the E2E latency (in milliseconds) for three simultaneous clients (*little3* + *hyang5* + *gates3*), employing different layouts and placement strategies. Latency was significantly lower and more consistent as the deployment scaled out when employing correlation grouping.

In order to further highlight the benefit of collocation, we disabled the object caching performed by each step of our application. Without caching, steps always have to fetch objects from the K/V store. In this context, the main difference between the random placement and correlation grouping strategies is that correlation grouping guarantees that objects being fetched are always stored locally, i.e. in the same Cascade node (and shard) where the computation is running. In the case of random placement, there is no guarantee: objects are placed randomly across shards.

Figure 6 shows the results comparing the two placement strategies with and without the application-level caching, for a workload of three simultaneous clients, and 3/5/5 shards (MOT/PRED/CD steps, respectively), one node per shard. Due to the zero-copy design of Cascade, E2E latency was the same with or without caching when employing correlation grouping, since memory copies are minimized and there is no serialization overhead when an UDL makes a get request to the same node where it is running: keeping objects in the application memory or fetching them locally from the K/V store incurs virtually the same cost. However, in the case of random placement, disabling caching significantly increased latency and reduced throughput. The median E2E latency was off-scale at more than 58 seconds, hence the bar for this case is replaced with an arrow. Throughput was on average 6.7 FPS, thus the pipeline was not able to handle the 7.5 FPS sent by clients collectively.

We also evaluated the impact of replication on the E2E latency of the application. Different layouts with more than one node per shard were employed for this evaluation. On Cascade, when a shard has more than one node, any object stored in that shard is replicated to all nodes in the shard, before any computation is triggered. As a result, any computation triggered in such a shard will have local access to the objects in that shard, even if the previous computation (e.g. state of the previous frame) was performed in another node. This behavior can be seen as a form of prefetching, since nodes store objects that will be used in the future before the corresponding request arrives. However it incurs extra latency since the corresponding computation is only triggered after the replication is completed, while a more sophisticated prefetching feature would not prevent the computation to start while prefetching is done in other nodes.

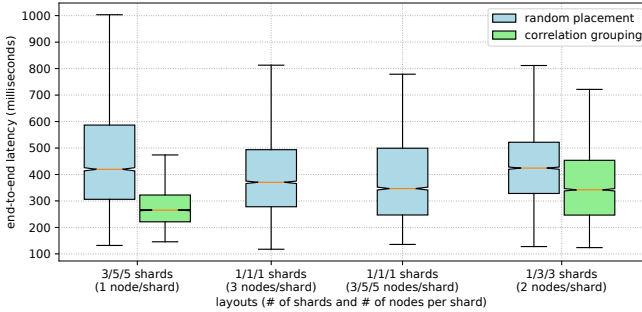


Figure 7. E2E latency with replication on Cascade.

Figure 7 shows results for different layouts. The first group of bars is presented as reference, and show the E2E latency for 3/5/5 shards, with one node per shard (no replication). The next two bars present results for 1/1/1 shards, with different number of nodes per shard (3 and 3/5/5), so there is no difference between random placement and correlation grouping. The last layout has 1/3/3 shards, with 2 nodes per shard, configuring a compromise between having many shards with just one node each and a single shard with many nodes. Results show that replication reduced latency compared to the baseline (first bar). However, employing correlation grouping and multiple shards still results in better E2E latency. We argue that these results show the potential of further investigating the integration of correlation grouping with prefetching and scheduling.

4.7 Insights

Correlation grouping significantly reduces the latency of the RCP application on Cascade, compared to other placement options Cascade is able to support. Additional benefits include better scalability than with random placement, where adding nodes sometimes degraded performance. Performance was steady across varied workloads, suggesting that correlation grouping improves hardware utilization. Changes to the application were primarily to register regular expressions (Table 1 during initialization, as illustrated in Figure 3). Support for correlation grouping required minor changes to Cascade itself, yet enabled the system to use correlation keys to place objects and route requests. Our results on replication indicate that there is potential to improve latency even further by integrating correlation grouping with prefetching.

5 RCP Deployment on a Public Cloud

A natural question to ask is whether our claim that existing SP and ML serving platforms are inadequate is correct. To address this, we now describe a second deployment of RCP on Microsoft Azure Cloud. Granted, Azure is a public cloud whereas Cascade primarily targets a private cluster, but we believe this is a fair comparison because it genuinely represents a state-of-the-art alternative.

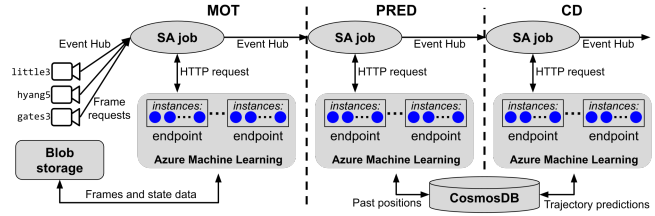


Figure 8. RCP deployment on Azure.

The goal of the section is to show evidence that: (i) data access patterns of applications such as RCP indeed result in extra fetching overheads; and (ii) although it is possible to overcome these overheads, it comes at the cost of a high coupling between application and deployment, since there is no unified mechanism available in modern platforms such as the proposed correlation grouping.

5.1 Deployment on Microsoft Azure Cloud

The RCP pipeline was implemented on Stream Analytics (SA) – Azure’s SP platform. We reused the source-code of each of the 3 steps (MOT, PRED, and CD), with few modifications. Each of the ML models was first configured on Azure Machine Learning (AML) as real-time endpoints, using a web-services interface. AML is elastic: depending on load, endpoints can be backed by worker instance pools of varying size [21]. Pipeline stages were connected using Azure Event Hubs (EHs) [14]. Clients were deployed in a virtual machine. Frames from all three videos were stored in Azure Blob Storage [4], which was also used to store MOT state data. Positions of agents and trajectory predictions are stored using Cosmos DB [27]. The resulting architecture is shown in Figure 8, and is compliant with recommendations from the cloud vendor. The individual ML tasks were properly configured with ample resources (similar to the resources employed previously in the Cascade experiments).

Clients stream video frames to the first SA job in the pipeline at a rate of 2.5 FPS, through an EH. The SA job invokes an MOT endpoint: one of the instances in the endpoint is selected by a load balancer to serve the request. The instance fetches the video frame from Blob storage and performs the inference (we assume the client has already uploaded the frame). The state from the previous frame is also fetched from Blob storage if it is not already cached in the instance’s memory. Results are sent through another EH to the next SA job responsible for invoking PRED endpoints for agent positions. For each invocation, the selected instance of the invoked PRED endpoint stores the new position on Cosmos DB, and also fetches the past positions of the corresponding agent that are not already cached in memory. The CD step is performed in a similar fashion. The final output of the pipeline is sent back to the client running on the virtual machine. End-to-end latency of a frame is the time elapsed from when the frame request was first sent by the client,

until the last output from the CD step for that frame was received by the client.

All instances in AML endpoints maintain MOT states, positions and trajectory predictions cached in memory for later reuse, thus avoiding fetching from Blob storage or Cosmos DB as much as possible. In the experiments reported in this section, we employ, for each step in the pipeline, a varying number of endpoints and instances per endpoint, as indicated. Instances in MOT and PRED endpoints were of type *Standard_NC4as_T4_v3* (equipped with NVIDIA T4 GPUs), while CD instances were of type *Standard_DS3_v2*.

We employed as many partitions in EHs and streaming units in SA as supported by the endpoints ($2 \times$ number of instances), maximizing parallelism [22]. The partition key for MOT requests was the video name, ensuring that frames originating in any single client were processed sequentially. Similarly, the partition key for PRED was the agent identifier, and for CD the frame number. We set the batch size when invoking AML endpoints to 1, a configuration intended to minimize per-frame latency.

Our experiments stream 700 frames, but we discard measurements the first 100 to give the framework time to warmup. Each experiment was repeated three times. To vary the workload (the number of simultaneous clients streams), we first tested with a single video at a time (*little3*, *hyang5*, and *gates3*), then with two concurrent video streams (*little3 + hyang5*), and finally with three (*little3 + hyang5 + gates3*).

5.2 Results: From One to Two Simultaneous Clients

We now report results for experiments with just one client, a case that establishes baseline latency for each video stream, processed individually in a heavily provisioned, dedicated infrastructure. In this set of experiments, each step of the application had one corresponding endpoint, and we varied the number of instances. The MOT endpoint had only one instance, while PRED and CD endpoints had 1, 3, and 5.

Figure 9 shows a box plot of the E2E latencies (in seconds) for each video and number of PRED/CD instances. The number of instances for PRED and CD endpoints is indicated on the horizontal axis. For *gates3*, the latency for 1 instance was significantly high and thus the bar was replaced by an arrow. The plot shows that increasing the number of instances from 1 to 3 reduced the median and 75th percentiles. However, no significant benefit was observed when increasing the number of instances to 5 for *little3* and *hyang5*. The reason for this is that 3 instances were enough to significantly parallelize invocations to PRED. Increasing the number of instances even further resulted in more network overhead of fetching agent positions that offset the gain of extra parallelism, since the rate of cache misses increased. With 3 instances, 64ms was spent per frame fetching data in the PRED step for *hyang5*, while 74ms was spent on average with 5 instances.

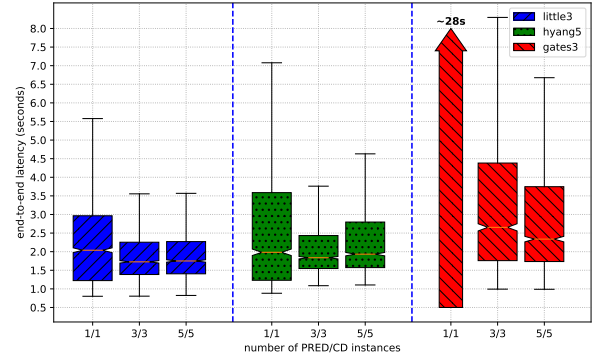


Figure 9. End-to-end latency for individual clients.

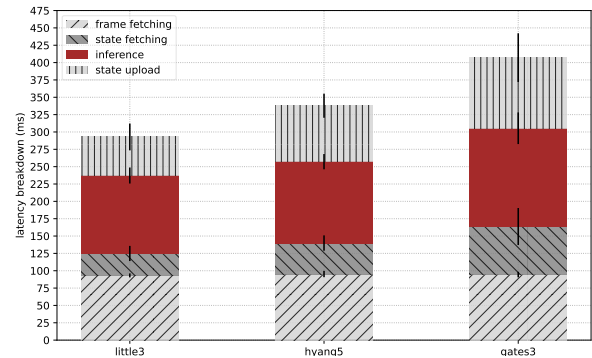


Figure 10. Latency breakdown of the MOT step.

We increased the workload to two simultaneous clients (*little3 + hyang5*), using the same configuration as the experiments above for individual clients. The average E2E latency, for 5 instances of PRED/CD, was about 67 seconds. The main reason for this significant increase in latency is that a single instance for the MOT step is inadequate to handle the increased rate of incoming frames (5 FPS in the aggregate from the two clients). It is necessary to increase the number of instances of the MOT endpoint.

We conducted experiments with two simultaneous clients, employing 5 instances for PRED and CD endpoints and a varying number of instances for the MOT endpoint (3, 5, 7, and 9). For 3 MOT instances, the E2E latency was significantly high. With 5 to 9 instances, the median latencies were all above 4 seconds, with similar distributions. The benefit of increasing the number of instances was limited, mainly due to the extra network overhead of fetching the MOT states. The extra delay causes requests to pile up in queues, resulting in a significantly higher E2E latency. Figure 10 shows a breakdown of the MOT step for each of the videos, when employing 3 instances on the MOT endpoint. The breakdown shows how much time was spent on average (in ms) on different MOT sub-steps: fetching the video frame, retrieving the state from the previous frame, inference, and uploading the state of the current frame.

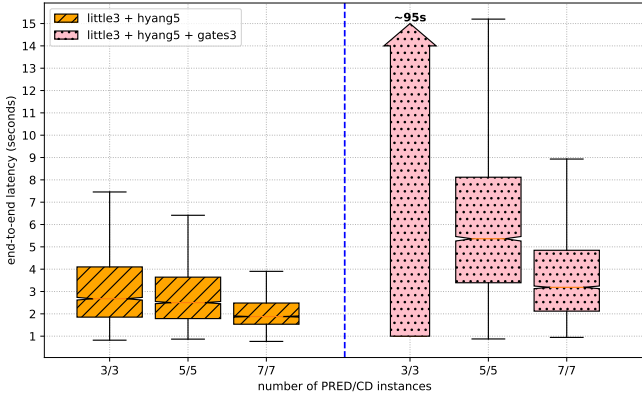


Figure 11. Grouped MOT with 2 and 3 simultaneous clients.

5.3 Results: Slashing Overheads From MOT

Since we know that the MOT step requires state data regarding frames from the same video, we deployed a separate MOT endpoint for each video, with one instance each. A separate SA job was also deployed for each endpoint, receiving requests from a separate EH. Then, each client sends requests to the corresponding EH. This ensures that frames from the same video will always be received by the same instance, avoiding the overhead of fetching states since they will be already in memory. We say that MOT step is now *grouped*. Figure 11 shows the E2E latency of two and three simultaneous clients, employing three MOT endpoints with one instance each, and a varying number of PRED and CD instances (3, 5, and 7). It is possible to see that latency became lower and more consistent as the number of instances for PRED and CD endpoints increased.

However, we observed that there is still potential to further cut network overheads. As we increased the number of PRED and CD instances, parallelism is increased, but so is the time spent fetching agent positions and trajectory predictions from Cosmos DB. Figure 12 shows the latency breakdown for PRED and CD steps, with three simultaneous clients, three grouped MOT endpoints, and a varying number of PRED and CD instances (3, 5, and 7). The plot shows the average time spent per frame (in ms) fetching the necessary input data and running the corresponding inference. The values shown are a sum of the measured times for all invocations. With 7 PRED/CD instances, for example, the average time spent fetching data per frame in PRED and CD steps was almost 200ms (roughly 100ms for each step).

5.4 Results: Slashing Overheads From PRED and CD

Here we employ the same approach as described above for MOT, leveraging application-specific knowledge to group PRED and CD. We deploy multiple endpoints with one instance each, instead of one endpoint with multiple instances. However, it is not possible to rely any longer on the endpoint

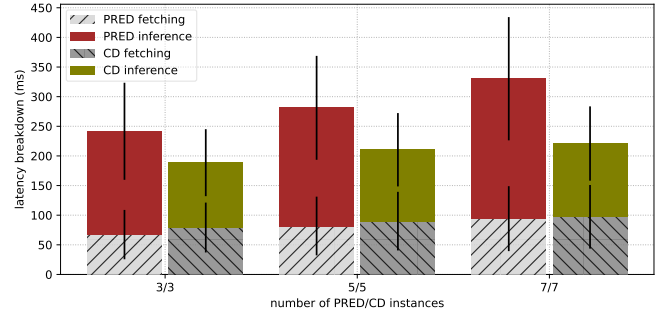


Figure 12. Latency breakdown of PRED and CD steps.

```

1 WITH mot_output AS (
2   SELECT [mot-little3-endpoint](input) AS res
3   FROM [from-little3-client] AS input
4 ), expanded_output AS (
5   SELECT r.arrayvalue.* FROM mot_output
6   CROSS APPLY GetArrayElements(res) AS r
7 )
8
9 SELECT * INTO [to-pred-0] FROM expanded_output
10 WHERE agent_id % num_pred_endpoints = 0
11
12 SELECT * INTO [to-pred-1] FROM expanded_output
13 WHERE agent_id % num_pred_endpoints = 1

```

Figure 13. Code excerpt from the MOT SA job for *little3*.

load balancer to select which instance will receive each request. Thus, we manually select in the SA jobs code which endpoint to forward each request, by writing the output of the previous step to the corresponding EH. For PRED, this selection was based on the agent identifier, modulo the number of PRED endpoints. For CD, the selection was based on the frame number, modulo the number of CD endpoints.

Figure 13 shows a code excerpt (simplified for the sake of presentation) from the SA job responsible for the MOT endpoint associated with the video *little3*. In the code, *from-little3-client* is an EH where the client responsible for the *little3* video sends requests. Function *mot-little3-endpoint* invokes the AML endpoint containing a single instance that performs the MOT inference. There are two queries (lines 9 and 12) that forwards the position of each agent to a specific EH (*to-pred-0* or *to-pred-1*) depending on the agent identifier and the number of PRED endpoints. The EHs *to-pred-0* and *to-pred-1* will deliver the agents positions to the corresponding SA jobs that will invoke their associated PRED endpoints.

Figure 14 shows a comparison between the pipeline with only the MOT step grouped and the pipeline with all three steps grouped. We varied the number of endpoints (with one instance each) for PRED and CD (3, 5, and 7, in different combinations), while MOT always had three endpoints (one for each video). As a workload, we configured three side-by-side client streams. Latency for 3 PRED/CD instances and only MOT grouped was significantly high (median 95 seconds) and was replaced by an arrow for the sake of presentation.

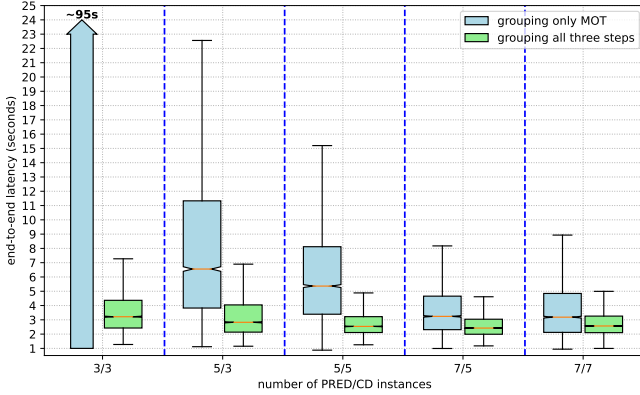


Figure 14. Grouping only MOT and grouping all steps.

It is possible to observe a significant benefit when grouping all three steps. The measured latency stabilizes with 5 PRED/CD instances, no benefit was observed when further adding more instances. The gain in parallelism was limited, however, we argue that more instances would be able to handle a heavier workload without an increase in latency.

5.5 Insights, Trade-offs, and Limitations

Without our manual grouping, scaling in Azure is straightforward: it is only necessary to increase the number of instances in AML, streaming units in SA, and/or partitions in EHs. AML endpoints will distribute requests across all the available instances automatically according to their load. Furthermore, it is possible to use auto-scaling features, which will scale the deployment in/out according to predefined metrics.

However, when employing the manual grouping strategy, scaling is done by adding or removing endpoints, which requires the application to be reconfigured. In the case of our deployment in Azure, changing endpoints affects client and SA jobs code, and it is also necessary to create new EHs. Load balancing and auto-scaling would need to be implemented by the application itself.

Despite all trade-offs, the benefit of grouping is significant, as also observed in Section 4. For MOT in particular, grouping was essential to support more than one client. Without grouping, the overhead of fetching states caused each MOT request to take more than 400ms, which is the time it takes for each client to send the next frame request. This caused requests to pile up in queues at the first step of the pipeline. In a time-pressured scenario such as the RCP application, the 400ms threshold is of high importance: the ML model employed in the PRED step predicts agents trajectories in the next 4.8 seconds. If it takes too long to process each frame, due to queuing, then the prediction may not be useful any longer. Furthermore, since the application handles a real-time video stream, the MOT state data for each frame will only be ever used once (for the following frame). However,

without grouping it is moved twice (upload and download), which can be considered wasteful.

Another clear benefit of grouping is better instance utilization. One could argue that each video/client configures a separate application which could be deployed separately, in a dedicated infrastructure. However, we showed that grouping allows multiple clients to share the same infrastructure while maintaining the same level of performance, which requires less instances to be deployed since they are better utilized. Furthermore, such shared deployment enables new clients to be dynamically added in runtime. However, this would require an extra front-end step in the pipeline that decides how the grouping of a new client should be performed (we’ve done it statically for our experiments).

6 Related Work

Prior efforts [1, 16, 17, 25, 26] argue for a *white box* approach, in which optimizations are employed in compilation or training time, based on specific features such as topology of neural networks. While such approaches can reduce the computational cost of model serving, our work employs a *black box* approach in which the application only needs to identify data / compute correlations. Although the authors in [17] criticize *black box* approaches, they focus only on caching, buffering and batching in non-pipelined applications. The correlation grouping mechanism can support all of these capabilities but also enables additional optimizations, such as proactive data/computation collocation and prefetching.

Existing systems offer a number of mechanisms to express application-specific knowledge and/or request grouping; these features can be found in Redis hash tag, Azure Cosmos DB, EHs and SA partition key, RDD *location preferences*, Apache Spark Streaming *partitions*, and Apache Storm *stream grouping*. However, as noted in Section 3, such mechanisms: (i) are highly coupled with deployment; (ii) do not collocate data and computation in a unified fashion; (iii) are not able to express all possible correlations between data and computation; and/or (iv) may have a non-negligible computational cost as the deployment scales out.

The Pheromone [36] system offers a novel approach that the authors refer to as a *data bucket* abstraction, in which the outputs of functions are automatically grouped into buckets. Developers can then arrange for downstream functions to use data buckets as inputs. This enables Pheromone to place functions close to where the data is stored. The data bucket abstraction is similar to correlation grouping, however outputs in data buckets are always volatile (once consumed, they are garbage collected). The correlation grouping approach is compatible with data persistence, and we would argue that this gives greater flexibility. For example, some outputs may be needed between separate invocations of a pipeline (e.g. past positions of agents in the PRED step of the RCP application); our approach covers such cases but the data bucket

model does not. Furthermore, the authors do not consider more complex workflows in which multiple functions may require access to the same output in different stages, or in which a function requires data located in multiple buckets.

Several works improve data locality by scheduling tasks where input data (or most of it) is located [2, 6, 23, 24, 32, 35, 38], or by scheduling tasks that interact with each other in the same location (node, VM, or container) [15, 18]. These solutions follow a reactive approach: data is first placed without taking into account their correlations, and then tasks are placed where “most of input data” is located. Due to the data access patterns of latency-sensitive ML pipelines, a proactive approach, such as enabled by correlation grouping, may be necessary. We claim that our proposed mechanism is complementary to scheduler-based solutions.

7 Conclusion

We proposed an correlation grouping mechanism that enables developers to express application-specific knowledge of data/computation correlations, and then for platforms to use this information to reduce latency and improve efficiency. Our results show that the proposed mechanism is able to maintain significantly lower and more consistent latency, as well as higher node utilization as the application workload increases and the infrastructure scales out.

Acknowledgments

We are grateful to Professor Luís Rodrigues for the insightful comments on early versions of this paper. Partial support for our work was provided by AFRL/Ry under the SWEC program, Microsoft, Nvidia and Siemens.

References

- [1] Zeeshan Ahmed, Saeed Amizadeh, Mikhail Bilenko, Rogan Carr, Wei-Sheng Chin, Yael Dekel, Xavier Dupre, Vadim Eksarevskiy, Senja Filipi, Tom Finley, Abhishek Goswami, Monte Hoover, Scott Inglis, Matteo Interlandi, Najeeb Kazmi, Gleb Krivosheev, Pete Lufrenko, Ivan Matantsev, Sergiy Matushevych, Shahab Moradi, Gani Nazirov, Justin Ormont, Gal Oshri, Artidoro Pagnoni, Jignesh Parmar, Prabhat Roy, Mohammad Zeeshan Siddiqui, Markus Weimer, Shaheen Zahirazami, and Yiwen Zhu. 2019. Machine Learning at Microsoft with ML.NET. In *Proceedings of the 25th ACM SIGKDD International Conference on Knowledge Discovery & Data Mining* (Anchorage, AK, USA) (KDD '19). Association for Computing Machinery, New York, NY, USA, 2448–2458. <https://doi.org/10.1145/3292500.3330667>
- [2] Eric Boutin, Jaliya Ekanayake, Wei Lin, Bing Shi, Jingren Zhou, Zhengping Qian, Ming Wu, and Lidong Zhou. 2014. Apollo: Scalable and Coordinated Scheduling for Cloud-Scale Computing. In *11th USENIX Symposium on Operating Systems Design and Implementation (OSDI 14)*. USENIX Association, Broomfield, CO, 285–300. <https://www.usenix.org/conference/osdi14/technical-sessions/presentation/boutin>
- [3] Mikel Broström. 2022. *Real-time multi-camera multi-object tracker using YOLOv5 and StrongSORT with OSNet*. https://github.com/mikelbrostrom/Yolov5_StrongSORT_OSNet
- [4] Brad Calder, Ju Wang, Aaron Ogus, Niranjan Nilakantan, Arild Skjolsvold, Sam McKelvie, Yikang Xu, Shashwat Srivastav, Jiesheng Wu, Huseyin Simitci, et al. 2011. Windows azure storage: a highly available cloud storage service with strong consistency. In *Proceedings of the Twenty-Third ACM Symposium on Operating Systems Principles*. 143–157.
- [5] Cheng Chen, Jun Yang, Mian Lu, Taize Wang, Zhao Zheng, Yuqiang Chen, Wenyuan Dai, Bingsheng He, Weng-Fai Wong, Guoan Wu, Yuping Zhao, and Andy Rudoff. 2021. Optimizing In-Memory Database Engine for AI-Powered on-Line Decision Augmentation Using Persistent Memory. *Proc. VLDB Endow.* 14, 5 (jan 2021), 799–812. <https://doi.org/10.14778/3446095.3446102>
- [6] Daniel Crankshaw, Gur-Eyal Sela, Xiangxi Mo, Corey Zumar, Ion Stoica, Joseph Gonzalez, and Alexey Tumanov. 2020. InferLine: Latency-Aware Provisioning and Scaling for Prediction Serving Pipelines. In *Proceedings of the 11th ACM Symposium on Cloud Computing* (Virtual Event, USA) (SoCC '20). Association for Computing Machinery, New York, NY, USA, 477–491. <https://doi.org/10.1145/3419111.3421285>
- [7] Daniel Crankshaw, Xin Wang, Guilio Zhou, Michael J. Franklin, Joseph E. Gonzalez, and Ion Stoica. 2017. Clipper: A Low-Latency Online Prediction Serving System. In *14th USENIX Symposium on Networked Systems Design and Implementation (NSDI 17)*. USENIX Association, Boston, MA, 613–627. <https://www.usenix.org/conference/nsdi17/technical-sessions/presentation/crankshaw>
- [8] Shuiguang Deng, Hailiang Zhao, Weijia Fang, Jianwei Yin, Schahram Dustdar, and Albert Y. Zomaya. 2020. Edge Intelligence: The Confluence of Edge Computing and Artificial Intelligence. *IEEE Internet of Things Journal* 7, 8 (2020), 7457–7469. <https://doi.org/10.1109/JIOT.2020.2984887>
- [9] Derecho Project. 2023. *Cascade*. <https://github.com/Derecho-Project/cascade>
- [10] Yunhao Du, Yang Song, Bo Yang, and Yanyun Zhao. 2022. Strongsort: Make Deepsort Great Again. *arXiv preprint arXiv:2202.13514* (2022).
- [11] John C Eidson, Mike Fischer, and Joe White. 2002. IEEE-1588™ Standard for a Precision Clock Synchronization Protocol for Networked Measurement and Control Systems. In *Proceedings of the 34th Annual Precise Time and Time Interval Systems and Applications Meeting*. 243–254.
- [12] Harshayu Girase. 2022. *Human Path Prediction*. <https://github.com/HarshayuGirase/Human-Path-Prediction>
- [13] Haruna Isah, Tariq Abughofa, Sazia Mahfuz, Dharmitha Ajerla, Farhana Zulkernine, and Shahzad Khan. 2019. A Survey of Distributed Data Stream Processing Frameworks. *IEEE Access* 7 (2019), 154300–154316. <https://doi.org/10.1109/ACCESS.2019.2946884>
- [14] Benjamin Kettner and Frank Geisler. 2022. IoT Hub, Event Hub, and Streaming Data. In *Pro Serverless Data Handling with Microsoft Azure: Architecting ETL and Data-Driven Applications in the Cloud*. Springer, 153–168.
- [15] Swaroop Kotni, Ajay Nayak, Vinod Ganapathy, and Arkaprava Basu. 2021. Faastlane: Accelerating Function-as-a-Service Workflows. In *2021 USENIX Annual Technical Conference (USENIX ATC 21)*. USENIX Association, 805–820. <https://www.usenix.org/conference/atc21/presentation/kotni>
- [16] Peter Kraft, Daniel Kang, Deepak Narayanan, Shoumik Palkar, Peter Bailis, and Matei Zaharia. 2020. Willump: A Statistically-Aware End-to-end Optimizer for Machine Learning Inference. In *Proceedings of Machine Learning and Systems*, I. Dhillon, D. Papailiopoulos, and V. Sze (Eds.), Vol. 2. 147–159. https://proceedings.mlsys.org/paper_files/paper/2020/file/d9e5bd751997cfa6bc2d0e31ebdc048-Paper.pdf
- [17] Yunseong Lee, Alberto Scolari, Byung-Gon Chun, Marco Domenico Santambrogio, Markus Weimer, and Matteo Interlandi. 2018. PRETZEL: Opening the Black Box of Machine Learning Prediction Serving Systems. In *13th USENIX Symposium on Operating Systems Design and Implementation (OSDI 18)*. USENIX Association, Carlsbad, CA, 611–626. <https://www.usenix.org/conference/osdi18/presentation/lee>
- [18] Ashraf Mahgoub, Edgardo Barsallo Yi, Karthick Shankar, Sameh El-nikety, Somali Chaterji, and Saurabh Bagchi. 2022. ORION and the

- Three Rights: Sizing, Bundling, and Prewarming for Serverless DAGs. In *16th USENIX Symposium on Operating Systems Design and Implementation (OSDI 22)*. USENIX Association, Carlsbad, CA, 303–320. <https://www.usenix.org/conference/osdi22/presentation/mahgoub>
- [19] Nantia Makrynioti and Vasilis Vassalos. 2021. Declarative Data Analytics: A Survey. *IEEE Transactions on Knowledge and Data Engineering* 33, 6 (2021), 2392–2411. <https://doi.org/10.1109/TKDE.2019.2958084>
- [20] Karttikeya Mangalam, Yang An, Harshayu Girase, and Jitendra Malik. 2021. From Goals, Waypoints & Paths to Long Term Human Trajectory Forecasting. In *Proceedings of the IEEE/CVF International Conference on Computer Vision (ICCV)*. 15233–15242.
- [21] Microsoft. 2022. *Integrate Azure Stream Analytics with Azure Machine Learning*. <https://learn.microsoft.com/en-us/azure/stream-analytics/machine-learning-udf>
- [22] Microsoft. 2022. *Leverage query parallelization in Azure Stream Analytics*. <https://learn.microsoft.com/en-us/azure/stream-analytics/stream-analytics-parallelization>
- [23] Philipp Moritz, Robert Nishihara, Stephanie Wang, Alexey Tumanov, Richard Liaw, Eric Liang, Melih Elibol, Zongheng Yang, William Paul, Michael I. Jordan, and Ion Stoica. 2018. Ray: A Distributed Framework for Emerging AI Applications. In *13th USENIX Symposium on Operating Systems Design and Implementation (OSDI 18)*. USENIX Association, Carlsbad, CA, 561–577. <https://www.usenix.org/conference/osdi18/presentation/moritz>
- [24] Robert Nishihara, Philipp Moritz, Stephanie Wang, Alexey Tumanov, William Paul, Johann Schleier-Smith, Richard Liaw, Mehrdad Niknami, Michael I. Jordan, and Ion Stoica. 2017. Real-Time Machine Learning: The Missing Pieces. In *Proceedings of the 16th Workshop on Hot Topics in Operating Systems (Whistler, BC, Canada) (HotOS '17)*. Association for Computing Machinery, New York, NY, USA, 106–110. <https://doi.org/10.1145/3102980.3102998>
- [25] Matteo Paganelli, Paolo Sottovia, Kwanghyun Park, Matteo Interlandi, and Francesco Guerra. 2023. Pushing ML Predictions Into DBMSs. *IEEE Transactions on Knowledge and Data Engineering* 35, 10 (2023), 10295–10308. <https://doi.org/10.1109/TKDE.2023.3269592>
- [26] Kwanghyun Park, Karla Saur, Dalitso Banda, Rathijit Sen, Matteo Interlandi, and Konstantinos Karanasos. 2022. End-to-End Optimization of Machine Learning Prediction Queries. In *Proceedings of the 2022 International Conference on Management of Data (Philadelphia, PA, USA) (SIGMOD '22)*. Association for Computing Machinery, New York, NY, USA, 587–601. <https://doi.org/10.1145/3514221.3526141>
- [27] Rob Reagan. 2018. *Cosmos DB*. Apress, Berkeley, CA, 187–255. https://doi.org/10.1007/978-1-4842-2976-7_6
- [28] Redis. 2023. *Scaling with Redis Cluster*. <https://redis.io/docs/management/scaling/>
- [29] Alexandre Robicquet, Amir Sadeghian, Alexandre Alahi, and Silvio Savarese. 2016. Learning Social Etiquette: Human Trajectory Understanding In Crowded Scenes. In *Computer Vision – ECCV 2016*, Bastian Leibe, Jiri Matas, Nicu Sebe, and Max Welling (Eds.). Springer International Publishing, Cham, 549–565.
- [30] Ted Shaowang, Nilesh Jain, Dennis D. Matthews, and Sanjay Krishnan. 2021. Declarative Data Serving: The Future of Machine Learning Inference on the Edge. *Proc. VLDB Endow.* 14, 11 (jul 2021), 2555–2562. <https://doi.org/10.14778/3476249.3476302>
- [31] Weijia Song, Yuting Yang, Thompson Liu, Andrea Merlina, Thiago Garrett, Roman Vitenberg, Lorenzo Rosa, Aahil Awatramani, Zheng Wang, and Ken Birman. 2022. Cascade: An Edge Computing Platform for Real-Time Machine Intelligence. In *Proceedings of the 2022 Workshop on Advanced Tools, Programming Languages, and PLatforms for Implementing and Evaluating Algorithms for Distributed Systems (Salerno, Italy) (APPLIED '22)*. Association for Computing Machinery, New York, NY, USA, 2–6. <https://doi.org/10.1145/3524053.3542741>
- [32] Vikram Sreekanti, Chenggang Wu, Xiayue Charles Lin, Johann Schleier-Smith, Joseph E. Gonzalez, Joseph M. Hellerstein, and Alexey Tumanov. 2020. Cloudburst: Stateful Functions-as-a-Service. *Proc. VLDB Endow.* 13, 12 (jul 2020), 2438–2452. <https://doi.org/10.14778/3407790.3407836>
- [33] Apache Storm. 2023. *Concepts*. <https://storm.apache.org/releases/current/Concepts.html>
- [34] Xiang Wang, Yang Hong, Harry Chang, Kyoungsoo Park, Geoff Langdale, Jiayu Hu, and Heqing Zhu. 2019. Hyperscan: A Fast Multi-pattern Regex Matcher for Modern CPUs. In *16th USENIX Symposium on Networked Systems Design and Implementation (NSDI 19)*. USENIX Association, Boston, MA, 631–648. <https://www.usenix.org/conference/nsdi19/presentation/wang-xiang>
- [35] Bowen Yu, Guanyu Feng, Huanqi Cao, Xiaohan Li, Zhenbo Sun, Haojie Wang, Xiaowei Zhu, Weimin Zheng, and Wenguang Chen. 2021. Chukonu: A Fully-Featured High-Performance Big Data Framework That Integrates a Native Compute Engine into Spark. *Proc. VLDB Endow.* 15, 4 (dec 2021), 872–885. <https://doi.org/10.14778/3503585.3503596>
- [36] Minchen Yu, Tingjia Cao, Wei Wang, and Ruichuan Chen. 2023. Following the Data, Not the Function: Rethinking Function Orchestration in Serverless Computing. In *20th USENIX Symposium on Networked Systems Design and Implementation (NSDI 23)*. USENIX Association, Boston, MA, 1489–1504. <https://www.usenix.org/conference/nsdi23/presentation/you>
- [37] Matei Zaharia, Mosharaf Chowdhury, Tathagata Das, Ankur Dave, Justin Ma, Murphy McCauly, Michael J. Franklin, Scott Shenker, and Ion Stoica. 2012. Resilient Distributed Datasets: A Fault-Tolerant Abstraction for In-Memory Cluster Computing. In *9th USENIX Symposium on Networked Systems Design and Implementation (NSDI 12)*. USENIX Association, San Jose, CA, 15–28. <https://www.usenix.org/conference/nsdi12/technical-sessions/presentation/zaharia>
- [38] Haoyu Zhang, Ganesh Ananthanarayanan, Peter Bodik, Matthai Philipose, Paramvir Bahl, and Michael J. Freedman. 2017. Live Video Analytics at Scale with Approximation and Delay-Tolerance. In *14th USENIX Symposium on Networked Systems Design and Implementation (NSDI 17)*. USENIX Association, Boston, MA, 377–392. <https://www.usenix.org/conference/nsdi17/technical-sessions/presentation/zhang>
- [39] Kaiyang Zhou, Yongxin Yang, Andrea Cavallaro, and Tao Xiang. 2022. Learning Generalisable Omni-Scale Representations for Person Re-Identification. *IEEE Transactions on Pattern Analysis and Machine Intelligence* 44, 9 (2022), 5056–5069. <https://doi.org/10.1109/TPAMI.2021.3069237>
- [40] Xuanhe Zhou, Chengliang Chai, Guoliang Li, and Ji Sun. 2022. Database Meets Artificial Intelligence: A Survey. *IEEE Transactions on Knowledge and Data Engineering* 34, 3 (2022), 1096–1116. <https://doi.org/10.1109/TKDE.2020.2994641>

A Application Workload

Figure 15 show the workload of each video (*little3*, *hyang5*, and *gates3*), as well as the aggregated workload for two simultaneous videos (*little3 + hyang5*), and three simultaneous videos (*little3 + hyang5 + gates3*). Workload is expressed in number of agents detected in each frame. It is possible to see that *little3* has the lowest workload across all 700 frames, while *gates3* has the highest – during the first half of the videos, there are more agents in *gates3* frames than in the aggregated *little3 + hyang5* frames.

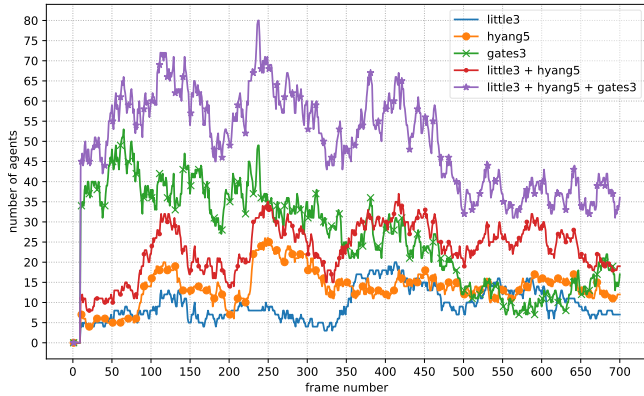


Figure 15. Number of agents for different workloads.

Figure 16 shows the size of the MOT state (in MBs) for each frame of each of the three videos employed in our experiments.

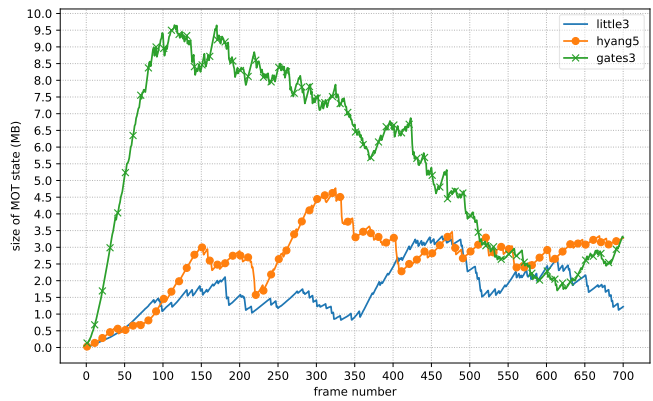


Figure 16. Size of the MOT state for each frame of each video.